

## Transition Metal Complexes with Mixed Nitrogen-Sulphur (N-S) Donor Macrocyclic Schiff Base Ligand: Synthesis, Spectral, Electrochemical and Antimicrobial Studies

Rayees Ahmad Shiekh<sup>1,\*</sup>, Ismail Ab Rahman<sup>1</sup>, Maqsood Ahmad Malik<sup>2</sup>, Norhayati Luddin<sup>1</sup>, Sam'an Malik Masudi<sup>1</sup>, Shaeel Ahmed Al-Thabaiti<sup>2</sup>

<sup>1</sup>School of Dental Sciences, Universiti Sains Malaysia, 16150 Kubang Kerian, Kelantan, Malaysia

<sup>2</sup>Department of Chemistry, Faculty of Science, King Abdulaziz University, P.O. Box 80203, Jeddah 21589, Saudi Arabia

\*E-mail: [rayeeschem@gmail.com](mailto:rayeeschem@gmail.com)

Received: 9 February 2013 / Accepted: 27 March 2013 / Published: 1 May 2013

---

A new mixed thia-aza-oxo macrocycle schiff base viz., 1,10-dithia-3,8,12,17-tetraoxo-4,7,13,16-tetraazacyclooctadecane with a series of transition metals Cu(II), Co(II), Ni(II) and Mn(II) has been synthesised by the [2+2] condensation of thiodiglycolic acid and ethylenediamine. Different techniques like FTIR, <sup>1</sup>H NMR, ESI MS, UV-Vis spectroscopy, conductivity and magnetic measurements were used to investigate the structural features of the synthesised compounds. Electronic absorption and IR spectra indicate octahedral geometry for chloro and nitrate complexes and square geometry for all sulphato complexes. The redox behaviour was investigated by cyclic voltammetry and show metal centered reduction process for all complexes. The reduction and oxidation potential depends on the structure and conformation of the central atom in the coordination compounds. The complexes of Cu(II) show both oxidation and reduction process. These metal complexes were also tested for their *in vitro* antimicrobial activities against some bacterial and fungal strains to assess their inhibiting potential and the activities shown by these complexes were compared with standard drugs.

---

**Keywords:** Schiff base, Complexes, N-S donor, Antimicrobial activities,

### 1. INTRODUCTION

The design and synthesis of well-arranged metal-containing macrocycles is an interesting field of macrocyclic synthetic chemistry [1,2]. In addition to their particular structural features,

supramolecular species formed by self-assembly of transition metals introduce many special functional and biological properties. The macrocyclic Schiff base ligands have received vital attention not only because of their pharmacological properties like antifungal, anticancer, antiviral, antibacterial character [3,4] and their mixed soft-hard donor character, versatile coordination behavior [5,6], but also for their capacity for chemical recognition of anions and metals of biochemical, medical and environmental importance [7,8]. In case of N and C based functionalized macrocyclic ligands, the mode of metal incorporation is very much similar to that of metalloproteins in which the requisite metal is bound in a macrocyclic cavity or cleft produced by the conformational arrangement of the protein [9]. The attachment of metal ions to proteins such as monoclonal antibodies can create new tools for use in biology and medicine [10]. This type of ligands has theoretical importance also because they are capable of furnishing an environment with controlled geometry and ligand field strength [11, 12]. The reagents used for such attachments are called bifunctional chelating agents [13]. They have shown to be efficient catalyst for cleavage of the phosphate ester bond [14]. The precise molecular recognition between macrocyclic ligands and their guest provides a good opportunity for studying key aspects of supramolecular chemistry, which are also significant in a variety of disciplines including chemistry, biology, physics, medicine and related science and technology [7]. The recent growing interest in the electrochemistry (reduction and oxidation process) of macrocyclic complexes derived from recognition of biological importance of the less common oxidation states of Cu and Ni [15, 16]. Redox potentials of Cu(II)/Cu(I) depends on the relative thermodynamic stabilities of the two oxidation states in a given ligand environment. The biological activities of the metal complexes may be associated to the redox properties of these complexes. Some Cu(II) compounds a lower reduction potential seems to be related to an increased antifungal activity [17,18]. *Candida albicans* is an opportunistic and often deadly pathogen that attacks host tissues, undergoes a dimorphic shift, and then grows as a fungal mass in the kidney, heart or brain. It is the fourth leading cause of hospital-acquired infection in the United States and over 95% of AIDS patients suffer from infections by *C. albicans* [19, 20]. *Candida albicans* is the predominant organism associated with candidiasis; but other *Candida* species, including *C. glabrata*, *C. tropicalis* and *C. krusei*, are now emerging as serious nosocomial threats to patient populations [21]. Existing antifungals can treat mucosal fungal infections but very few treatments are available for invasive diseases. The current antifungal therapy suffers from drug related toxicity, severe drug resistance, non-optimal pharmacokinetics, and serious drug-drug interactions. The common antifungal drugs currently used in clinics belong to polyenes and azoles. Polyenes (amphotericin B and nystatin) cause serious host toxicity [22] whereas azoles are fungistatic and their prolonged use contributes to the development of drug resistance in *C. albicans* and other species [23, 24]. Because of all these striking problems, there is a pressing need to develop novel antifungal drugs with higher efficiency, broader spectrum, improved pharmacodynamic profiles and lower toxicity. Moreover, it is considered of interest to incorporate other chemotherapeutically-active group within the structure, hoping to impart some synergism to the target compounds. Hydrazones are organic compounds characterized by the presence of  $-\text{NH}-\text{N}=\text{CH}-$  group in their molecule. Acyl-hydrazones have an additional donor site like  $\text{C}=\text{O}$ , which determine the versatility and flexibility of these compounds. Such molecules show anticonvulsant, anti-inflammatory, analgesic, antimicrobial, antitumor, anti-platelet, and antiviral properties [25]. The aim of the present work is to report synthesis, characterization and antimicrobial

studies of a 1,10-dithia-3,8,12,17-tetraoxo-4,7,13,16-tetraazacyclooctadecane Schiff base ligand and its transition metal complexes, which can be used as high potential drug. In addition we have studied the electrochemical behaviour of these synthesized complexes by cyclic voltammetry.

## 2. EXPERIMENTAL

All the chemicals used were of analytic grade, and were procured from Aldrich. Metal salts were purchased from E. Merck and were used as received. All solvents used were of standard/spectroscopic grade.

### 2.1. Physical measurements

All synthesis and handling were carried out under an atmosphere of dry and oxygen-free nitrogen using standard Schlenk techniques and samples for microanalysis were dried in vacuum to constant weight. Thiodiglycolic acid, ethylenediamine were received from Merck and used as supplied. The solvents were also purchased from Merck and were used without further purification. Elemental analyses were performed by a Perkin Elmer 2400 CHNSO Elemental Analyser. FT-IR spectra of solid samples were recorded on a Perkin Elmer Spectrum 100 FT-IR spectrometer (Universal/ATR Sampling Accessory). Bruker DPX-300 MHz spectrophotometer was used to record  $^1\text{H}$  NMR spectra at room temperature with DMSO  $d_6$  as solvent. The chemical shift ( $\delta$ ) are reported in parts per million (ppm) using tetramethylsilane as internal standard. Positive and negative ESI mass spectra were measured by Bruker (esquire3000-00037) instrument. Magnetic susceptibility measurements were approved out from a microanalysis laboratory by Gouy method at room temperature. Electronic spectra were recorded on a spectro-UV-Vis Dual Beam 8 auto cell UVS-2700 LABOMED, INC, US spectrophotometer using DMSO as solvent. Melting points (mp) was recorded on a Metrex melting point apparatus and the results are uncorrected. Before the electrochemical experiments, the electrodes were dried with an argon gas stream and the solutions were purged with pure argon gas (99.999 %) at least for 10 min and an argon atmosphere was maintained over the solution during experiments. Electrochemical performance of the metal complexes was measured with CH Instruments, U.S.A (Model 1110A-Electrochemical analyzer, Version 4.01) in HPLC grade DMF containing  $n\text{-Bu}_4\text{NClO}_4$  as the sustaining electrolyte. The three-electrode system consisted of glassy carbon electrode (3 mm diameter) as a working electrode, a Ag/AgCl (3 M KCl) reference electrode and a platinum wire as auxiliary electrode was used. In order to provide a reproducible active surface and to improve the sensitivity and resolution of the voltammetric peaks, the glassy carbon electrode was polished to a mirror finish with 0.3 micron alumina on a smooth polishing cloth and then rinsed with methanol and double distilled water prior to each electrochemical measurements. The electrode cleaning procedure requires less than 3 min. All measurements were carried out at room temperature (24  $^{\circ}\text{C}$ ).

## 2.2. Synthesis of Macrocyclic Schiff base

### Ligand 1,10-dithia-3,8,12,17-tetraoxo-4,7,13,16-tetraazacyclooctadecane

The warm ethanolic solution (25 ml), of thiodiglycolic acid (3.0 g, 0.02 mol.) and a warm ethanolic solution (25 ml) of ethylenediamine (3.00 g, 0.05 mol) were mixed slowly with constant stirring. This mixture was refluxed at 60-70 °C for 7-8 h in the presence of few drops of concentrated hydrochloric acid. On keeping it at 0 °C, overnight, a white cream precipitate was formed, which was filtered, washed with cold ethanol and dried in vacuo over P<sub>4</sub>O<sub>10</sub> and it was recrystallised from methanol (yield 69%), mp. 170 °C, IR (KBr, cm<sup>-1</sup>): 3289(N-H), 2990(C-H), 1645(C=O), 1440(C-N), 1022, 868, 761; <sup>1</sup>H NMR (300 MHz, δ ppm from TMS in DMSO-d<sub>6</sub>, 300 k): δ 9.31-8.95 (4H, br CO-N-H), δ 4.35- 4.47(8H, C-H<sub>2</sub>), δ 2.74- 2.83(8H, OC-N-C-H<sub>2</sub>). ESI MS (m/z) 348 [M]<sup>+</sup>, 349 [M+1]<sup>+</sup>. Elem anal calcd C 41.36, H 5.79, O 18.37, N 16.08, S 18.40%; found C 41.39, H 5.81, O 18.39, N 16.10, S 18.42%.

## 2.3. Synthesis of metal complexes

A hot ethanolic (20 ml) solution of the corresponding metal salts (0.001 mol.) was added to a hot ethanolic (20 ml) suspension of the macrocyclic ligand (0.001 mol). The mixture was stirred for 7 hours at 30 °C and the solution was reduced to half of its volume. It was then allowed to stand overnight in a refrigerator. A coloured complex precipitated out, which was secluded by filtration under vacuum. It was washed systematically with cold ethanol and dried in vacuo over P<sub>4</sub>O<sub>10</sub>.

## 2.4. Antimicrobial Activity

### 2.4.1. Growth Conditions

Stock cultures of *Candida albicans* ATCC 10261, *Candida tropicalis* ATCC 750, *Candida glabrata* ATCC 90030 and *Candida krusei* ATCC 6258 were maintained on slants of nutrient agar (yeast extract 1%, peptone 2%, D-glucose 2% and agar 2.5%) (HiMedia) at 4 °C. To initiate growth for experimental purposes, one loop full of cells from an agar culture was inoculated into 25ml of respective nutrient media and incubated at 30-37 °C for 24 hr i.e. up to stationary phase (primary culture). The cells from primary culture (10<sup>8</sup> cells ml<sup>-1</sup>) were re-inoculated into 100 ml fresh YEPD medium and grown for 8-10 h i.e., upto mid-log phase (10<sup>6</sup> cells ml<sup>-1</sup>). Stock cultures of *Pseudomonas* were cultured in King's B media while as that of *E. coli* were cultured in Maconky agar. Fluconazole and Ampicillin were purchased from SIGMA chemicals (USA).

### 2.4.2. Determination of MIC<sub>80</sub>

MIC<sub>80</sub> was determined *in vitro* in liquid medium by serial broth dilution method [26]. Standard drugs Fluconazole and Ampicillin were included as positive controls. The MIC values keep up a correspondence to the most minuscule concentrations that did not allow for the recognition of any visible growth.

## 2.4.3. Disc Diffusion Assay

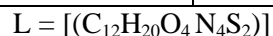
Inhibitory activity of ligand, its metal complexes and standard drugs against different microbes was determined by Disc Diffusion Method [27].

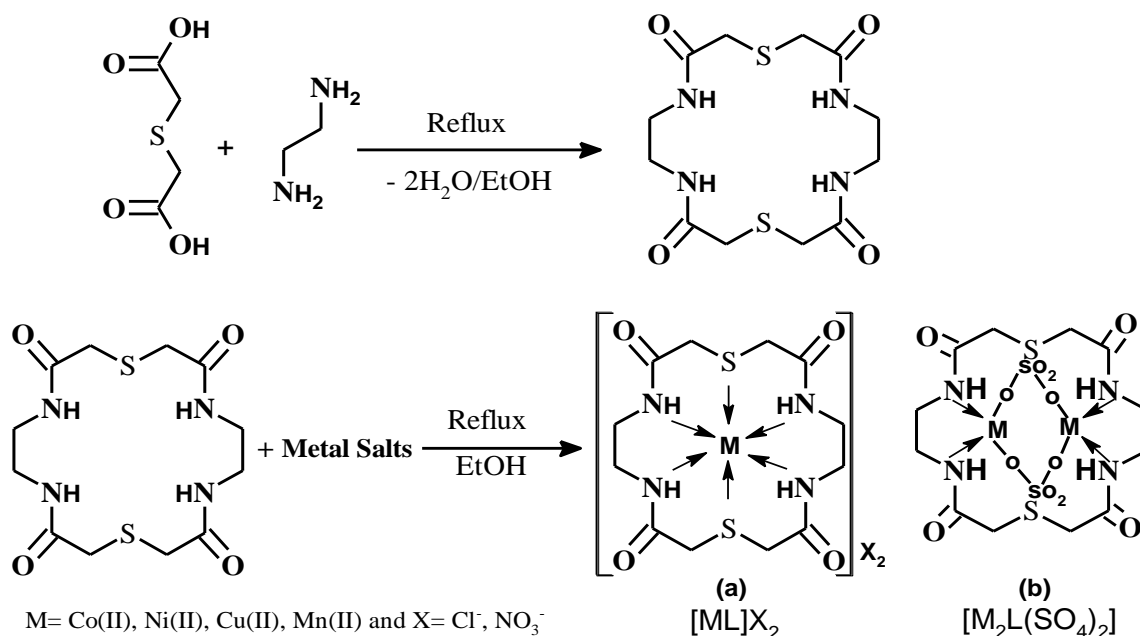
## 3. RESULTS AND DISCUSSION

On the basis of elemental analyses, the complexes were assigned the composition shown in Table 1. The analytical data of the complexes correspond well with the general formula  $[ML]X_2$  and  $[M_2L(SO_4)_2]$  where L = macrocyclic ligand; M = Co(II), Cu(II), Ni(II) and Mn(II), and X =  $Cl^-$ ,  $NO_3^-$ . The molar conductance indicates that the all complexes are 1:2 electrolytes in nature except sulphato complexes which are non-electrolytic in nature. The ligand was synthesized by condensing the corresponding acid and the diamine with few drops hydrochloric acid (scheme 1). This ligand was then refluxed at room temperature with the metal salts to form their corresponding metal complexes (scheme 1 a, b).

**Table 1.** Analytical data and Physical properties of the complexes

Complexes molecular formula	Colour	Yield (%)	Molar Conductance ( $\Omega^{-1}cm^2 mol^{-1}$ )	M.P. ( $^{\circ}C$ )	Mol. Wt Found (Cal.) %	Molecular weight Found (Calculated) %				
						M	C	H	N	O
[CoL]Cl <sub>2</sub>	Pink	62	260	215	475 (477.83)	8.00 (8.10)	30.31 (30.13)	4.21 (4.18)	11.78 (11.74)	13.47 (13.40)
[CoL](NO <sub>3</sub> ) <sub>2</sub>	Mauve pink	60	250	210	529 (530.93)	8.97 (9.00)	27.22 (27.12)	3.78 (3.76)	10.58 (10.55)	12.09 (12.06)
[Co <sub>2</sub> L(SO <sub>4</sub> ) <sub>2</sub> ]	Red	58	10	250	655 (657.86)	11.11 (11.16)	21.98 (21.96)	3.05 (3.01)	8.54 (8.50)	9.77 (9.74)
[NiL]Cl <sub>2</sub>	Green	63	215	210	476 (477.59)	8.11 (8.13)	30.25 (30.21)	4.20 (4.16)	11.76 (11.72)	13.44 (13.39)
[NiL](NO <sub>3</sub> ) <sub>2</sub>	Light green	59	220	205	582 (530.69)	8.99 (9.04)	27.27 (27.25)	3.78 (3.72)	10.60 (10.57)	12.12 (12.10)
[Ni <sub>2</sub> L(SO <sub>4</sub> ) <sub>2</sub> ]	Light green	60	10	255	655 (657.38)	11.16 (11.20)	21.98 (21.96)	3.05 (3.02)	8.54 (8.51)	9.77 (9.75)
[CuL]Cl <sub>2</sub>	Royal blue	64	260	220	480 (482.44)	7.55 (7.59)	30.00 (29.98)	4.16 (4.12)	11.66 (11.62)	13.33 (13.30)
[CuL](NO <sub>3</sub> ) <sub>2</sub>	Greenish blue	60	245	210	532 (535.54)	8.37 (8.42)	27.06 (27.04)	3.75 (3.70)	10.52 (10.49)	12.03 (12.00)
[Cu <sub>2</sub> L(SO <sub>4</sub> ) <sub>2</sub> ]	Blue	58	10	250	664 (667.08)	10.45 (10.49)	21.68 (21.64)	3.01 (3.00)	8.43 (8.40)	9.63 (9.60)
[MnL]Cl <sub>2</sub>	Light brown	65	250	235	470 (473.83)	8.53 (8.62)	30.63 (30.60)	4.25 (4.22)	11.91 (11.89)	13.61 (13.59)
[MnL](NO <sub>3</sub> ) <sub>2</sub>	Light brown	60	255	230	524 (526.93)	9.53 (9.59)	27.48 (27.46)	3.81 (3.79)	10.68 (10.65)	12.21 (12.19)
[Mn <sub>2</sub> L(SO <sub>4</sub> ) <sub>2</sub> ]	Brown	58	10	250	647 (649.86)	11.77 (11.83)	22.25 (22.21)	3.09 (3.07)	8.65 (8.60)	9.89 (9.86)





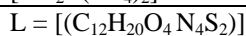
**Scheme 1 (a, b):** Synthesis of macrocyclic ligand and its metal complexes.

### 3.1. Infrared Red Spectra

An IR spectrum of ligand does not show any evidence of the band corresponding for the free primary diamine and hydroxyl group [28].

**Table 2.** Relevant IR spectral peaks (cm<sup>-1</sup>) and their assignments

Complexes	ν N-H	Amide bands			ν M-N	ν M-Cl
		I	II	III		
[CoL]Cl <sub>2</sub>	3255	1639	1215	770	449	345
[CoL](NO <sub>3</sub> ) <sub>2</sub>	3135	1636	1244	825	451	...
[Co <sub>2</sub> L(SO <sub>4</sub> ) <sub>2</sub> ]	3102	1642	1248	803	446	...
[NiL]Cl <sub>2</sub>	3152	1635	1240	730	450	352
[NiL](NO <sub>3</sub> ) <sub>2</sub>	3147	1638	1253	705	451	...
[Ni <sub>2</sub> L(SO <sub>4</sub> ) <sub>2</sub> ]	3115	1660	1232	710	410	...
[CuL]Cl <sub>2</sub>	3149	1644	1239	712	420	355
[CuL](NO <sub>3</sub> ) <sub>2</sub>	3178	1633	1225	719	428	...
[Cu <sub>2</sub> L(SO <sub>4</sub> ) <sub>2</sub> ]	3165	1645	1231	706	430	...
[MnL]Cl <sub>2</sub>	3160	1634	1236	695	450	340
[MnL](NO <sub>3</sub> ) <sub>2</sub>	3185	1639	1250	712	436	...
[Mn <sub>2</sub> L(SO <sub>4</sub> ) <sub>2</sub> ]	3170	1658	1238	709	427	...



Absence of a broad absorption band characteristic for hydroxyl group in acid indicates that the OH group of acid was detached from the COOH group to form a bond between carboxyl carbon atom and amino group, also suggest complete condensation of reactants. The appearance of new bands characteristics for amide groups at 1642 ν (C=O), amide I, 1530 ν (C-N) + δ (N-H), amide II, 1285 δ

(N-H), and  $645\text{ cm}^{-1}$   $\nu$  (C=O), amide III (Table 2). A sharp band observed in the region  $3370\text{--}3175\text{ cm}^{-1}$  may be assigned to  $\nu$ (N-H) of the secondary amino group [29].

The shifting in the band of  $\nu$ (C-N) towards the lower wave number in the metal complexes indicates that the coordination takes place through the nitrogen of the  $\nu$ (C-NH) group. This designates that the flow of electron density towards the metal atom is through the C-N group. This has been finally established through far IR spectra by the appearance of new signals seen at 340, 345, 352, 355,  $\text{cm}^{-1}$  in the spectra of metal complexes which gives us clear proof for the presence of metal-nitrogen bond in Mn(II), Co(II), Ni(II), and Cu(II) complexes respectively [30-32]. A strong to medium intensity band in the region of  $755\text{--}785\text{ cm}^{-1}$  has been assigned to  $\nu$ (C-S). The  $\nu$ (C-S) band is shifted by ca.  $35\text{ cm}^{-1}$  in the complexes which clearly indicate that sulphur also takes place in coordination.

### 3.2. $^1\text{H}$ NMR Spectra

The NMR spectrum of the ligand is consistent with the single species present in the solution, since only one set of signals is observed in the ligand.  $^1\text{H}$  NMR spectrum of the ligand shows a sharp signal in the range 8.90- 9.30 ppm which is attributed to amide CO-NH, (4H) [33, 34] and does not show any signal corresponding to primary amine. A signal appearing in the range 2.69- 2.80 ppm has been ascribed to methylene protons OC-N-CH<sub>2</sub>, (8H), while as C-H<sub>2</sub> (8H) protons appear in the range 4.20- 4.40 ppm. These proton signals undergo down field shifting in all the metal complexes of the macrocyclic ligand, because of the paramagnetic effect of metal (II) ions and hence support the coordination of the ligand towards the metal ions [35,36] and also the macrocyclic nature of the product.

### 3.3. Electro Spray Ionization Mass Spectra (ESI MS)

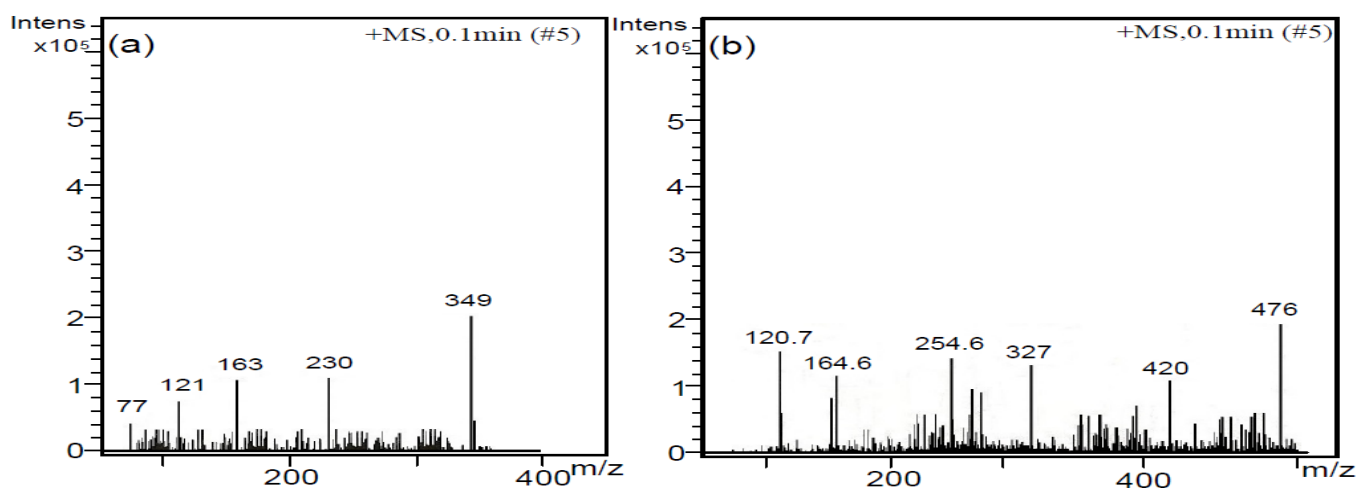


**Figure 1.** Electro Spray Ionization Mass Spectra (ESI MS) of (a) Ligand (L) and (b) Ni[(L)]Cl<sub>2</sub> complex.

A positive ion ESI mass spectrum of macrocyclic ligand confirms the proposed formula by showing a peak at  $m/z$  349 corresponding to the moiety  $[(C_{12}H_{20}O_4 N_4 S_2)]$  atomic mass  $m/z$  348] Fig. 1(a). The series of peaks in the range  $m/z$  77, 121, 163, 230 etc, may be assigned to various fragments. These data suggests the 2+2 condensation of succinic acid and ethylenediamine. Their intensity gives an idea of stability of fragments.  $[M+2]^+$  fragments were observed in all the metal complexes, possibly due to presence of isotopic chlorine in low quantities [36]. In some cases, the molecular ion peak was also associated with the solvent, water molecules and some adduct ions from the mobile phase solution [37, 38].

### 3.4. Bands due to anions

The IR spectra of nitrate complexes indicate that the nitrate group is uncoordinated as the strong band of free nitrate is present in the region of  $1375\text{--}1390\text{ cm}^{-1}$ . Thus, the nitrate group is not coordinated and it is present outside the sphere in all complexes [29]. The IR spectra of sulphato complexes of Co(II), Ni(II) and Cu(II) complexes the  $\nu_3$  and  $\nu_4$  split in the region of  $1095\text{--}1055$  (3 s) ( $\nu_3$ ) and  $640\text{--}575\text{ cm}^{-1}$  ( $\nu_4$ ) into three bands. These results suggest that, the symmetry is further lowered and reduced to  $C_{2v}$  and indicates bidentate nature of sulphate group [29]. Thus sulphate group acts as bridging bidentate group.

#### 3.4.1. Cobalt (II) complex

The magnetic moment of all the complexes except sulphato complex lie in the range of 4.96–5.06 B.M. corresponding to three unpaired electrons. The value of magnetic moments depends upon the amount of total orbital angular momentum and total spin angular momentum. The sulphato complexes show magnetic moment 1.96 B.M. corresponding to one unpaired electron [39, 40].

**Table 3.** Magnetic moment and electronic spectral data of the complexes

Complexes	$\mu_{\text{eff}}$ (B.M) <sup>a</sup>	Spectral bands $\lambda_{\text{max}}$ ( $\text{cm}^{-1}$ )
[CoL]Cl <sub>2</sub>	4.96	10450, 14750, 21135
[CoL](NO <sub>3</sub> ) <sub>2</sub>	5.06	10398, 16950, 23650
[Co <sub>2</sub> L(SO <sub>4</sub> ) <sub>2</sub> ]	1.96	9753, 22530
[NiL]Cl <sub>2</sub>	2.94	10250, 16738, 20990
[NiL](NO <sub>3</sub> ) <sub>2</sub>	3.02	10092, 17352, 22320
[Ni <sub>2</sub> L(SO <sub>4</sub> ) <sub>2</sub> ]	Diamagnetic	10050, 16852, 21995
[CuL]Cl <sub>2</sub>	1.96	13763, 18690, 20433
[CuL](NO <sub>3</sub> ) <sub>2</sub>	2.01	13220, 18422
[Cu <sub>2</sub> L(SO <sub>4</sub> ) <sub>2</sub> ]	0.70	14230, 18650, 23500
[MnL]Cl <sub>2</sub>	5.87	18549, 22783, 28110, 38662
[MnL](NO <sub>3</sub> ) <sub>2</sub>	5.92	17950, 21552, 26950
[Mn <sub>2</sub> L(SO <sub>4</sub> ) <sub>2</sub> ]	2.02	16530, 20550, 22358

L =  $[(C_{12}H_{20}O_4 N_4 S_2)]$ , <sup>a</sup> Error limit  $\pm 5\%$



Cobalt(II) complex exhibits absorption bands in region of 10180-10450 ( $\nu_1$ ), 14750-17680 ( $\nu_2$ ) and 21135-26750 ( $\nu_3$ )  $\text{cm}^{-1}$ , listed in Table 3. These bands may be assigned to  ${}^4\text{T}_{1g}(\text{F}) \rightarrow {}^4\text{T}_{2g}(\text{F})$ ,  ${}^4\text{T}_{1g} \rightarrow {}^4\text{A}_{2g}$  and  ${}^4\text{T}_{1g}(\text{F}) \rightarrow {}^4\text{T}_{1g}(\text{P})$  transitions respectively. Suggesting an octahedral geometry around Cobalt(II) ion [41]. The electronic spectra of the sulphato complexes show a narrow band at 9753 and a broader band at 22,530  $\text{cm}^{-1}$ , which correspond to square planar geometry [41].

### 3.4.2. Copper (II) complex

The magnetic moment of all the Cu(II) complexes recorded at room temperature lie in the range 1.96–2.02 B.M. This reveals that these complexes are monomeric in nature and also shows the absence of metal–metal interaction along the axial positions. Whereas, the  $[\text{Cu}_2\text{L}(\text{SO}_4)_2]$  type complex show magnetic moment at 0.70 B.M. indicates the presence of metal-metal interaction between them. Electronic spectra of six-coordinate Cu(II) complexes have either  $\text{D}_{4h}$  or  $\text{C}_{4v}$  symmetry, and eg and  $t_{2g}$  level of  ${}^2\text{D}$  free ion term will split into  $\text{B}_{1g}$ ,  $\text{A}_{1g}$ ,  $\text{B}_{2g}$  and  $\text{E}_g$  level, respectively. Thus, the three spin allowed transitions are estimated in the visible and near IR region. But only few complexes are known [42] in which such bands are determined either by Gaussian Analysis or single crystal polarisation studies. These bands may be assigned to following transitions,  ${}^2\text{B}_{1g} \rightarrow {}^2\text{A}_{1g}$ , ( $d_{x^2-y^2} \rightarrow d_z^2$ ) ( $\nu_1$ ),  ${}^2\text{B}_{1g} \rightarrow {}^2\text{B}_{2g}$ , ( $d_{x^2-y^2} \rightarrow d_{zy}$ ) ( $\nu_2$ ), and  ${}^2\text{B}_{1g} \rightarrow {}^2\text{E}_g$ , ( $d_{x^2-y^2} \rightarrow d_{zy}, d_{yz}$ ) ( $\nu_3$ ) in order of increasing energy. The electronic spectra of the complexes having molecular formula  $[\text{CuL}]\text{X}_2$  (where  $\text{X}=\text{Cl}^-$ ,  $\text{NO}_3^-$ ) show two bands in the range of 13,763–14,486  $\text{cm}^{-1}$ , 18,690–18,850  $\text{cm}^{-1}$  and 20,433–21,550  $\text{cm}^{-1}$  assignable to  ${}^2\text{B}_{1g} \rightarrow {}^2\text{A}_{1g}$ ,  ${}^2\text{B}_{1g} \rightarrow {}^2\text{B}_{2g}$  and  ${}^2\text{B}_{1g} \rightarrow {}^2\text{E}_g$  transitions, respectively. This suggests that these complexes have tetragonal geometry [41]. The electronic spectra of sulphato complexes with these ligands correspond to square planar geometry [43-45].

### 3.4.3. Nickel (II) complex

The positive ion ESI mass spectra of the nickel complex confirm the mononuclear complex by showing a peak at  $m/z$  476 Fig. 1(b). The magnetic moment of the Ni(II) complex at room temperature lie in the range of 2.94-3.02 B. M. These values fall in high spin configuration [40] and confirm the presence of an octahedral environment around the Ni(II) ion. The complex with molecular formula  $[\text{Ni}_2\text{L}(\text{SO}_4)_2]$  is diamagnetic suggesting square planar geometry. Electronic spectra of  $[\text{NiL}]\text{X}_2$  complexes (where  $\text{X}=\text{Cl}^-$ ,  $\text{NO}_3^-$ ) show bands in the region of 10250–10484  $\text{cm}^{-1}$ , 16738–16787  $\text{cm}^{-1}$  and 20990–21600  $\text{cm}^{-1}$ . These bands may be assigned to  ${}^3\text{A}_{2g}(\text{F}) \rightarrow {}^3\text{T}_{2g}(\text{F})$  ( $\nu_1$ ),  ${}^3\text{A}_{2g}(\text{F}) \rightarrow {}^3\text{T}_{1g}(\text{F})$  ( $\nu_2$ ), and  ${}^3\text{A}_{2g}(\text{F}) \rightarrow {}^3\text{T}_{1g}(\text{P})$  ( $\nu_3$ ), respectively. It suggests octahedral geometry of Ni(II) complexes [41]. The electronic spectra of sulphato complex show bands at 10,050, 16,852 and 21, 995  $\text{cm}^{-1}$  assignable to following  ${}^1\text{A}_{1g} \rightarrow {}^1\text{A}_{2g}$  ( $\nu_1$ ),  ${}^1\text{A}_{1g} \rightarrow {}^1\text{B}_{2g}$  ( $\nu_2$ ) and  ${}^1\text{A}_{1g} \rightarrow {}^1\text{E}_g$  ( $\nu_3$ ) transitions, respectively, corresponding to square planar geometry.

### 3.4.4. Manganese (II) complex

The room temperature magnetic moment of the Mn (II) complexes lies in the range 5.87–5.92BM corresponding to five unpaired electrons. Electronic spectra of Mn(II) complexes exhibit four

weak intensity absorption bands in the range 18,549–19,785 ( $\epsilon = 46\text{--}47 \text{ L mol}^{-1} \text{ cm}^{-1}$ ), 22,783–24,374 ( $\epsilon = 51\text{--}53 \text{ L mol}^{-1} \text{ cm}^{-1}$ ), 28,110–28,429 ( $\epsilon = 58\text{--}59 \text{ L mol}^{-1} \text{ cm}^{-1}$ ), and 38,662–38,810  $\text{cm}^{-1}$  ( $\epsilon = 74\text{--}76 \text{ L mol}^{-1} \text{ cm}^{-1}$ ). These bands may be assigned to the transitions:  ${}^6A_{1g} \rightarrow {}^4T_{1g}$  ( ${}^4G$ ),  ${}^6A_{1g} \rightarrow {}^4E_g$ ,  ${}^4A_{1g}$  ( ${}^4G$ ) and  ${}^6A_{1g} \rightarrow {}^4E_g$  ( ${}^4D$ ),  ${}^6A_{1g} \rightarrow {}^4T_{1g}$  ( ${}^4P$ ), respectively [46].

### 3.5. Cyclic voltammetric study (CV)

The electrochemical properties of the metal complexes, particularly with sulphur donor atoms have been studied in order to consider spectral and structural changes accompanying electron transfer. The redox properties include oxidation and reduction of the central metal ion, various oxidation and reduction reactions of the ligand, and processes which involve both the central atom and the ligand.

The cyclic voltammetric properties of Co(II) complexes were studied in the range from +1.5 to –2.0V. The electrochemical behaviour of all the cobalt(II) complexes were same even sulphato complexes having different geometry proposed from spectroscopic data for these complexes. Cyclic voltammogram of [CoL]Cl<sub>2</sub> shows a quasi-reversible peak for the couple: cobalt(II)→cobalt(III) at  $E_{pa} = 1.07\text{V}$  with the direct cathodic peak for cobalt(III)→cobalt(II) at  $E_{pc} = 0.87\text{V}$  (Fig. 2a). Two peaks exhibits, corresponding to cobalt(II)→cobalt(I) at  $E_{pc} = -1.22\text{V}$  and cobalt(I)→cobalt(0) at  $E_{pc} = -1.57\text{V}$  in the cyclic scan region of 0 to –2.0V. In the anodic region it also exhibits two peaks shows their oxidation of cobalt(0) → cobalt(II). Voltammetric parameters are studied in the scan rate interval of 50–800 $\text{mVs}^{-1}$ . The ratio between the cathodic peak current and the square root of the scan rate ( $I_{pc}/v^{1/2}$ ) is approximately constant. The peak potential shows a small dependence with the scan rate. The ratio  $I_{pa} - I_{pc}$  is close to unity. From these data, it can be concluded that this redox couple is related to a quasireversible one-electron transfer process controlled by diffusion.

The electrochemical behaviour of all the Ni(II) complexes are similar in the same conditions and depends on the potential range. On scanning from 0.0 to –2.0V (Fig. 2b), the cyclic voltammogram of [NiL]Cl<sub>2</sub> shows two waves in the cathodic scan at –0.99 and –1.56V, corresponds to reduction of the Ni(II) ion and in the reverse scan two anodic peaks at –1.54 and 1.02V. The redox couple are studied in the interval of 50–800 $\text{mVs}^{-1}$  shows a linear variation of  $I_{pc}/v^{1/2}$ . It show small dependence of the potential peak with scan rate is observed [47, 48], and again  $I_{pa} - I_{pc}$  ratio is close to unity. These suggests a diffusion controlled quasireversible Ni(II) – Ni(I) process. In sulphato complex of nickel it is difficult to have access +1 state for nickel when ligand in neutral form. The positive values of the oxidation process show that it is easier to oxidize as compared to reduce.

The electrochemical properties of the Cu(II) complexes were carried out in the range from +1.5 to –2.0V both the ranges of potentials were studied independently. The cyclic voltammogram between +1.5 and 0.0V shows oxidation process Cu(III)/Cu(II). While in the range of 0.0 to –2.0V it shows the reduction processes which may be assigned Cu(II)/Cu(I) and Cu(I)/Cu(O) processes. The voltammogram of copper complexes between +1.5 and 0.0V shows cathodic peak in the region of +1.23V and in forward scan at +0.795V. They give anodic peak near +1.14V associated with cathodic peak at 0.810 V (Fig. 2c). The  $\Delta E_p$  values lies in the range of 60–80mV, and the scan rate in vary in the range of 50–800 $\text{mVs}^{-1}$ , the ratio between the cathodic peak current and square root of the scan rate

( $L_{pc}/v^{1/2}$ ) is also constant. All of them resemble of a quasireversible one-electron transfer process [49, 50]. Cyclic scan in the range of 0 to  $-2.0V$  reveals peak at  $-0.73$  and  $-1.13V$  in the cathodic scan and the forward scan shows a peak at  $-0.670V$  associated with cathodic peak at  $-1.10V$ . These peaks correspond to successive Cu(II) reduction processes. The voltammogram of chloro and nitrate complexes are quite similar [51].

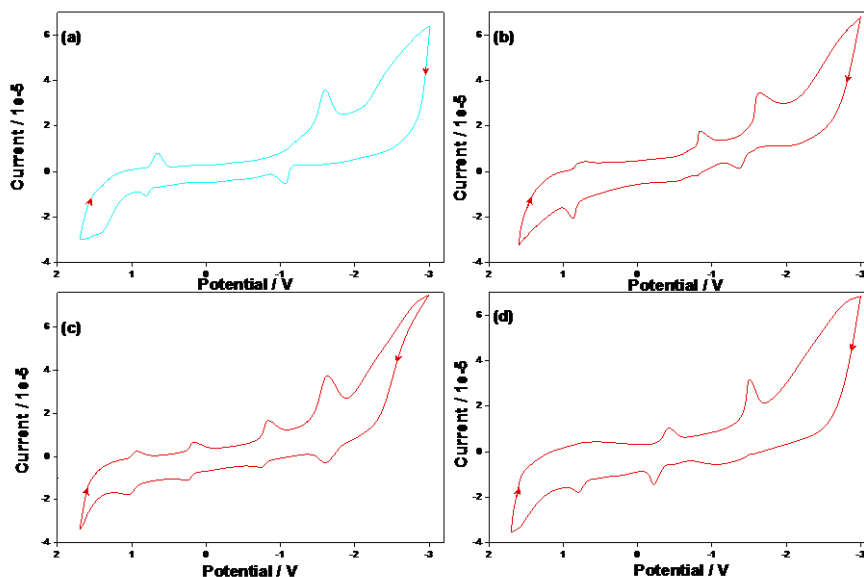


**Figure 2.** Cyclic voltammogram of: (a) Co(II), (b) Ni(II), (c) Cu(II), and (d) Mn(II) Metal Complexes

The redox property of the Mn(II) complex was studied in the potential range of  $+1.8$  to  $-2.0V$ . The Mn(II) complex is electroactive with respect to the metal center and exhibited two redox processes, each reduction is associated with a single-electron transfer process at room temperature [52, 53]. For both responses, the cathodic and anodic peak heights are equal, and vary as the square root of the scan rate;  $E_{pc}$  and  $E_{pa}$  are virtually independent of the scan rate. Two well-defined quasi-reversible one-electron cyclic responses were observed at  $E_{pc} = -1.28$  with a corresponding oxidation peak at  $E_{pa} = -0.56$  V and at  $E_{pc} = -0.65$  with a corresponding oxidation peak at  $E_{pa} = 0.91V$  respectively at a scan rate of  $100mV/s$ . The electrochemical behavior shows moderately high reduction potentials.  $\Delta E_p$  values for the first redox couple,  $0.83V$  is higher than for the second redox couple,  $0.25V$ .  $E_p$  value is higher for the complex due to the difference between the original complex and the reduced species. (Fig. 2d).

### 3.6. Antimicrobial Screening

#### 3.6.1. Minimum Inhibitory Concentration ( $MIC_{80}$ )

The  $MIC_{80}$  of ligand, its metal complexes and standard drugs were investigated against four fungal and two bacterial species using broth dilution method (BDM). In case of *Candida tropicalis*,

Ni(II) complex has MIC<sub>80</sub> which is 66% less as compared to parent compound, where as Mn(II), Co(II) and Cu(II) complexes have MIC<sub>80</sub> which is 62%, 58% and 55% less as compared to the original compound. From the results shown in (Fig. 3), it has been calculated that, in fungi generally the MIC<sub>80</sub> of S<sub>Ni</sub><S<sub>Mn</sub><S<sub>Co</sub><S<sub>Cu</sub><S, where as in case of bacteria the MIC<sub>80</sub> of S<sub>Co</sub><S<sub>Ni</sub><S<sub>Mn</sub><S<sub>Cu</sub><S. It was found that Ni(II) complex and standard drugs showed significant and identical inhibitory properties

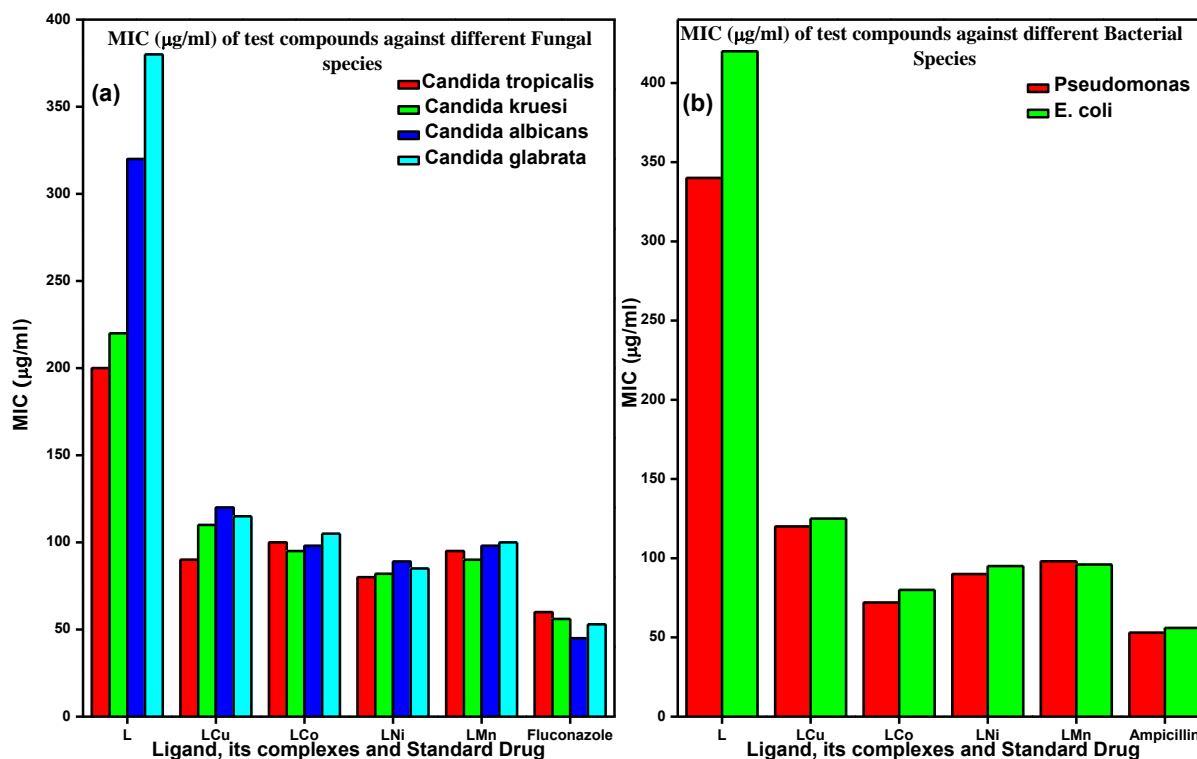


**Figure 3.** Minimum Inhibitory Concentrations MIC<sub>80</sub> (µg/ml) of ligand and its metal complexes against different (a) Fungal species and (b) Bacterial species.

### 3.6.2. Disc Diffusion Assay

The *in vitro* antibacterial activity of the ligand and its metal complexes were tested against two different bacteria at a concentration of 1000 µg/ml (10 fold more than MIC) Fig. 4(a). At this concentration the metal complexes show significant antimicrobial activity against the tested pathogens. The degree of inhibition varied with the nature of the compound. These concentrations of the ligand and complexes were used to get visible results. The highest zone of inhibition *i.e.* 18 and 16 mm were measured in *Pseudomonas* and *E.coli* when treated with Co(II), and again 16 mm measured in *E.coli* when treated with Ni(II) complex. The zone of inhibition is greatly affected by the thickness of the test agar layer. As the thickness increases, the zone of inhibition decreases. This can be attributed to the decrease of concentration of the ligand and its complexes per unit volume of the culture media. Another factor, which influences the inhibition zone, is inoculum size (concentration of the organism per unit volume). The diameter of the inhibition zone decreases with increase in the inoculum size. The

chemical composition, temperature of the incubator, and the pH of the medium influence the rate of germination of microorganisms.

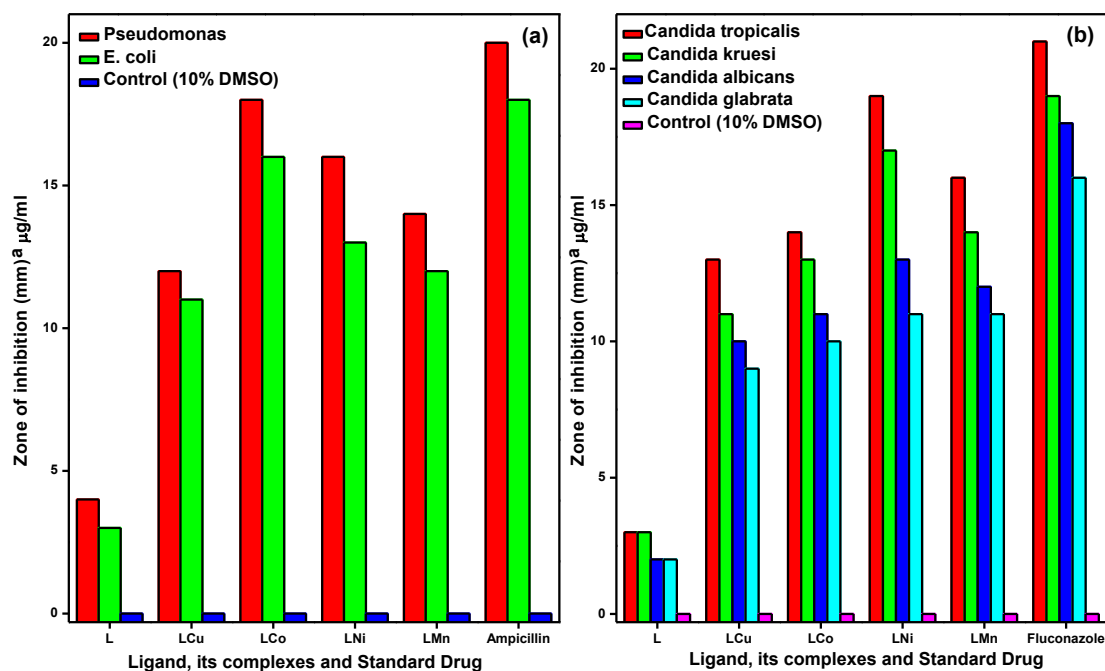


**Figure 4.** Bar diagram showing (a) antibacterial screening activity and (b) antifungal screening activity of the ligand and its metal complexes. <sup>a</sup>12-22 mm significant active, 06-12mm moderate active, < 06 less active. Ampicillin (negative control). Fluconazole (negative control). (10% DMSO) = Solvent control. L = [(C<sub>12</sub>H<sub>20</sub>O<sub>4</sub>N<sub>4</sub>S<sub>2</sub>)]

There is a significant reduction in the growth rate of microorganisms due to unfavorable culture media, low temperature and acidic pH. The activity test was conducted at an optimum temperature of 37 °C and favorable pH 0.2, both antifungal and antibacterial activities was calculated as a mean of three triplicates. Synthesized compounds were investigated for their antimicrobial activity by agar diffusion method [54]. Antifungal activity was also checked at the same concentrations (1000µg/ml) the highest inhibitory zone *i.e.* 19, 16 and 17 mm were measured in *Candida tropicalis*, *Candida kruesi* and *Candida tropicalis* when treated against Ni(II), Mn(II) and Ni(II) complexes (Fig.4(b)). The most significant results observed in this study were that the metal complexes were more active against fungi than in case of bacteria. In case of solvent control disc no zone of inhibition was observed as far as our study is concerned 10% DMSO, as a solvent is having no effect on the tested organisms. Hence we can effectively conclude here that whole of the antimicrobial effect is due to the different concentration of the metal complexes and the ligand used in this study. The antimicrobial behavior of the complexes when compared with standard antifungal and antibacterial drugs showed momentous and identical biological properties [55, 56].

Due to the high antimicrobial activities and chelation of these metal ions in their complexes, which enhances the lipophylic character favoring its permeation through the lipid layer of cell

membrane and the presence of favorable structural environment such as aryl binding site with a hydrophobic group, hydrogen bonding domain –NHCO– group, and nucleophiles present in these complexes. These metal complexes within the glass ionomer cement seem to be feasible to improve the properties of the regular cement. Regrettably, although the dental cements fill the gap between the tooth and the crown, bacterial micro leakage may occur, resulting in secondary caries. To overcome these failures, efforts have been made on developing new incorporated low molecular weight antibacterial agents. In future these ligands and their metal complexes can be used in the synthesis of modified Glass ionomer cements, because of their highly enhanced antimicrobial properties.

#### 4. CONCLUSION

In this paper, we describe the spectroscopic and biological studies of a new mixed thia-aza-oxo macrocycle schiff base ligand and its Mn(II), Co(II), Ni(II), and Cu(II) complexes. On the basis of spectral studies an octahedral geometry for chloro and nitrate complexes and square planar geometry for all sulphato complexes have been assigned. The antimicrobial screening data confirm that the metal chelates exhibit a higher inhibitory effect than the free ligand. Present observations may serve as a guide for studying the control release of these complexes that could be a promising future in the field of infectious diseases. As far as our results are concerned these metal complexes can thus be explored in future as an alternative for decreasing pathogenic potential of infecting bacterial and fungal species. The redox behaviour was explored by cyclic voltammetry based on the metal-centered reduction processes for all complexes.

#### ACKNOWLEDGEMENT

The authors would like to thank Ministry of Higher Education for financial support of this research grant scheme (FRGS, Grant No. 203/PPSG/6171138).

#### References

1. T. Fekner, J. Gallucci, M.K. Chan, *J. Am. Chem. Soc.* 126 (2004) 223.; R. A. Sheikh, S. Shreaz, L. A. Khan, A. A. Hashmi, *J. Chem. Pharm. Res.*, 2 (2010) 274.
2. J.L. Sessler, E. Katayev, G.D. Pantos, Y.A. Ustynuk, *Chem. Commun.* (2004) 1276; S. Chandra, N. Gupta, L.K. Gupta, *Synth. React. Inorg. Met.-Org. Chem.* 34 (2004) 919.
3. M. Wang., I.F. Wang, Y.Z. Li, Z.D. Xu, *Tran. Met. Chem.*, 26 (2001) 307.; R. A. Sheikh, S. Shreaz, L. A. Khan, A. A. Hashmi, *J. Chem. Pharm. Res.*, 2 (2010) 274.; A.M. Asiri, S.A. Khan, *Molecules* 15 (2010) 4784.
4. R. A. Shiekh, I. A. Rahman, M. A. Malik, S. M. Masudi, N. Luddin, *Int. J. Electrochem. Sci.*, 7 (2012) 12829.; R. A. Sheikh, S. Shreaz, L. A. Khan, A. A. Hashmi, *J. Chem. Pharm. Res.*, 2 (2010) 172.; A.M. Asiri, S.A. Khan, *Molecules* 15 (2010) 6850.
5. M. Maji, M. Chatterjee, S. Ghosh, S.K. Chattopadhyay, B.M. Wu, T.C.W. Mak, *J. Chem. Soc. Dalton Trans.* (1999) 15.

6. P. Sengupta, R. Dinda, S. Ghosh, W.S. Sheldrick, *Polyhedron* 22 (2003) 477.; R.R. Fenton, R. Gauci, P.C. Junk, L.F. Lindoy, R.C. Luckay, G.V. Meehan, J.R. Price, P. Tumer, G. Wei, *J. Chem.Soc. Dalton Trans.* (2002) 2185.
7. E. Labisbal, A. Sousa, A. Castineiras, A. Gracia-Vazquez, J. Romero, D.X. West, *Polyhedron*, 19, (2000) 1255.; M.K. Srivastava, B. Mishra, M. Nizamuddin, *Ind. J. Chem.*, 40B (2001) 342.
8. D.K. Dermertzi, N. Kourkoumelis, M.A. Dermertzis, J.R. Miller, C.S. Frampton, J. K. Swearingen, D.X. West, *Eur. J. Inorg. Chem.*, (2000) 727. M. Canadas, E. Lopez-Torres, A.M. Arias, M.A. Mandiola, M.T. Sevilla, *Polyhedron* 19 (2000) 2059
9. E.Q. Gao, H.Y. Sun, D.Z. Liao, Z.H. Jiang, S.P. Yan, *Polyhedron* 21 (2002) 359.
10. C.F. Meeres, T.G. Wensel, *Ace. Chem. Res.* 17 (1984) 202.
11. J. Gao, A.E. Martell, *Inorg. Chim. Acta* 122 (2002) 329.
12. S. Chandra, L.K. Gupta, D. Jain, *Spectrochim. Acta A* 60 (2004) 2411.
13. A.K. Mishra, J.F. Chatal, *New J. Chem.* 25 (2001) 336; L. Broge, I. Sotofte, C.E. Olsen, J. Springborg, *Inorg. Chem.* 40 (2001) 3124.
14. V. Alexander, *Chem. Rev.* 95 (1995) 273.
15. J.A. Streeky, D.G. Pillsburg, D.H. Busch, *Inorg. Chem.* 19 (1980) 3148.
16. A.A. Isse, A. Gennaro, E. Vianello, *J. Chem. Soc., Dalton Trans.* (1993) 2091.
17. D.X. West, E. Liberta, S.B. Padhye, R.C. Chikate, P.B. Sonawane, A.S. Kumbar, R.S. Yeranda, *Coord. Chem. Rev.* 123 (1993) 49.
18. Y. Haiduc, A. Silvestru, *Coord. Chem. Rev.* 99 (1990) 253.
19. H. Chi, Y. Yang, S. Shang, K. Chen, K. Yeh, F. Chang, J. Lin, *J. Microbiol. Immunol. Infect.* 44 (2011) 369.
20. P.L. Fidel, *Adv. Dent. Res.* 19 (2006) 80.
21. M.A. Pfaller, D.J. Diekema, *J. Clinic. Microbiol.* 42 (2004) 4419.
22. B. Cohen, *Int. J. Pharm.* 162 (1998) 95.
23. D. Sanglard, *Curr. Opinion Microbiol.* 5 (2002) 379.
24. K.A. Marr, T.C. White, J.A. van Burik, R.A. Bowden, *Clin. Infect. Dis.* 25 (1997) 908.
25. M.A. Malik, S.A. Al-Thabaiti, M.A. Malik, *Int. J. Mol. Sci.* 13 (2012) 10880.
26. K.G. Davey, A. Szekely, E.M. Johnson, D.W. Warnock, *J. Antimicrob. Chemotherapy.*, 42 (1998) 439.
27. K. Mukhopadhyay, A. Kohli, R. Prasad, *Antimicrob. Agents Chemotherapy.*, 46 (2002) 3695.
28. S. Chandra, L.K. Gupta, D. Jain, *Spectrochimica Acta A.*, 60 (2004) 2411.
29. K. Nakamoto. *Infrared spectra of Inorganic and Coordination Compounds*, Wiley Interscience, New York. (1970) 90.
30. M. Shakir, S.P. Varkey, P.S. Hamid. *Polyhedron.*, 12 (1993) 2775.
31. M. Shakir, K.S. Islam, A.K. Mohamed, M. Shagufta, S.S. Hasan, *Trans. Met. Chem.*, 24 (1999) 577.
32. F.M.A.M. Aqra, *Trans. Met. Chem.*, 24 (1999) 337.
33. P.S. Kalsi, *Spectroscopy of Organic Compounds*, fourth ed., New Age International (P) Ltd., New Delhi 1999.
34. S.C. Rawle, C.P. Moore, N.W. Alcock, *J. Chem. Soc. Dalton Trans.*, (1992) 2755.
35. R.M. Silverstein, F.X. Webster, *Spectroscopic Identification of organic Compounds*, 6th Edn, John Wiley and Sons. Inc. New York. (1998) 482.
36. W. Kemp, *Organic Spectroscopy*, Macmillan Press Ltd 1975.
37. M. Yamashita, J.B. Fenn, *J. Phy. Chem.*, 88 (1984) 4451.
38. M. Mann, *Organic Mass spectrometry.*, 25 (1990) 575.
39. R.L. Carlin, *Transition Metal Chemistry*, 1, Marcel Dekker, Inc., New York 1965.
40. S. Chandra, L.K. Gupta, *Spectrochimica Acta A.*, 60 (2004) 2767.
41. A.B.P. Lever, *Inorganic Electronic Spectroscopy*, (Second ed.), Elsevier, Amsterdam 1984.
42. S. Chandra, S.D.Sharma., *J. Indian Chem. Soc.*, 79 (2002) 495

43. E. Konig, *Structure and Bonding*, (Berlin: Springer Verlag), (1971) 175.
44. B.N. Figgis, *Introduction to ligand fields* (New Delhi: Willey Eastern) 1976.
45. A.A.A. Emara, M.I.A. Omima, *Trans. Met. Chem.*, 32 (2007) 889.
46. C. Preti, G. Tosi, *Aust. J. Chem.*, 20 (1976) 543.
47. P. Bindu, M.R.P. Kurup, T.R. Satyakeerty, *Polyhedron.*, 18 (1998) 321.
48. E. Pereira, L. Gomez, B. Castro, *Inorg. Chim. Acta* 271 (1998) 83; S. Chandra, L.K. Gupta, *J. Saudi Chem. Soc.* 8 (2004) 85.
49. A. Arquero, M.A. Mendiola, P. Souza, M.T. Sevilla, *Polyhedron.*, 15 (1996) 1657.
50. S. Chandra, L.K. Gupta, D. Shukla, *J. Saudi Chem. Soc.* 8 (2003) 331
51. N. Raman, A. Kulandaisamy, A. Shunmugasundaram, K. Jeyasubramanian, *Trans. Met. Chem.*, 26 (2001) 131.
52. M. Donzello, D. Dini, G. Arcangelo, C. Ercolani, R. Zhan, Z. Ou, P. Stuzhiz, K.J. Kadish, *J. Am. Chem. Soc.*, 125 (2003) 14190.
53. B.W. Rossister, J.F. Hamilton, *Physical Method of Chemisty*, 2nd Ed.; Wiley: New York, (1985) p.2.
54. R. A. Sheikh, S. Shreaz, M. A. Malik, L. A. Khan, A. A. Hashmi, *J. Chem. Pharm. Res.*, 2 (2010) 133.
55. S. Shreaz, R. A. Sheikh, R. Bhatia, K. Neelofar, S. Imran, A. A. Hashmi, N. Manzoor, S. F. Basir, L. A. Khan, *Biometals.*, 24 (2011) 923.
56. S. Shreaz, R.A. Sheikh, B. Rimple, A.A Hashmi, M. Nikhat, L.A. Khan, *Microbial Pathogenesis.*, 49 (2010) 75.